ELSEVIER

Journal of Molecular Catalysis A: Chemical 111 (1996) 67–79

JOURNAL OF MOLECULAR CATALYSIS A: CHEMICAL

Binuclear zirconocene cations with μ-CH_3-bridges in homogeneous Ziegler–Natta catalyst systems

Stefan Beck [a], Marc-Heinrich Prosenc [a], Hans-Herbert Brintzinger [a,*], Ralf Goretzki [b], Norbert Herfert [b], Gerhard Fink [b]

[a] *Fakultät für Chemie, Universität Konstanz, D-78343 Konstanz, Germany*
[b] *Max-Planck-Institut für Kohlenforschung, D-45466 Mülheim / Ruhr, Germany*

Received 22 December 1995; accepted 29 April 1996

Abstract

Binuclear zirconocene cations are observed by ^{1}H-NMR in C_6D_6 solutions containing $B(C_6F_5)_3$ and an excess of a zirconocene dimethyl complex. The CH_3-bridged cation $[((C_5H_5)_2ZrCH_3)_2(\mu\text{-}CH_3)]^+$, solvent-separated from the anion $H_3C\text{–}B(C_6F_5)_3^-$, is present in equilibrium with $(C_5H_5)_2Zr(CH_3)_2$ and the mononuclear ion pair $[(C_5H_5)_2ZrCH_3^+ \cdots H_3C\text{–}B(C_6F_5)_3^-]$; in more concentrated solutions, a binuclear ion pair $[((C_5H_5)_2ZrCH_3)_2(\mu\text{-}CH_3)^+ \cdots H_3C\text{–}B(C_6F_5)_3^-]$ is the dominant species. Similar equilibria are observed in C_6D_6 solutions containing $B(C_6F_5)_3$ and $(CH_3)_4C_2(C_5H_4)_2Zr(CH_3)_2$, $(CH_3)_2Si(C_5H_4)_2Zr(CH_3)_2$ or rac-$(CH_3)_2$Si(indenyl)$_2$Zr$(CH_3)_2$. Complexes with sterically more demanding ligands, such as $(C_5(CH_3)_5)_2Zr(CH_3)_2$ or rac-$(CH_3)_2$Si(2-methyl-benz[e]indenyl)$_2$Zr$(CH_3)_2$ do not form any binuclear species under these conditions. In the catalyst system rac-$(CH_3)_2$Si(indenyl)$_2$Zr$(CH_3)_2$/$Bu_3NH^+B(C_6F_5)_4^-$, activities for the polymerization of propene increase with excess of the dimethyl zirconocene complex. This effect is due in part to a sacrifice of some dimethyl zirconocene for the removal of impurities from the catalyst system and in part to a stabilization of the catalyst in the form of the binuclear cation $[((CH_3)_2Si(indenyl)_2ZrCH_3)_2(\mu\text{-}CH_3)]^+$. The latter appears to act, in the presence of propene, as a source of the mononuclear cation $[(CH_3)_2Si(indenyl)_2ZrCH_3(C_3H_6)]^+$, rather than as a polymerization catalyst by itself.

Keywords: NMR; Ziegler–Natta; Zirconocene

1. Introduction

The generation of active olefin polymerization catalysts from zirconocene dialkyl complexes by reaction with a strong Lewis acid, A, is generally considered to involve equilibria between the dialkyl complex $(C_5H_5)_2ZrR_2$ and its Lewis-acid adduct $(C_5H_5)_2Zr(R)R \cdot A$, which is equivalent to a contact ion pair between a zirconocene alkyl cation and the weakly coordinating anion $R\text{–}A^-$, $[(C_5H_5)_2ZrR^+ \cdots R\text{–}A^-]$, and of this species with an olefin-complexed, separated ion pair, $[(C_5H_5)_2ZrR(\text{olefin})]^+ R\text{–}A^-$ according to Eqs. (1) and (2) [1–6].

$$(C_5H_5)_2ZrR_2 + A \rightleftharpoons [(C_5H_5)_2ZrR^+ \cdots R\text{–}A^-] \quad (1)$$

$$[(C_5H_5)_2ZrR^+ \cdots R\text{–}A^-] + \text{olefin} \rightleftharpoons [(C_5H_5)_2ZrR(\text{olefin})]^+ + R\text{–}A^-. \quad (2)$$

* Corresponding author. Fax: (+49-7531) 883137.

1381-1169/96/$15.00 Copyright © 1996 Elsevier Science B.V. All rights reserved.
PII S1381-1169(96)00168-9

More recently, evidence has been obtained that binuclear cations of the type $[((C_5H_5)_2MCH_3)_2(\mu\text{-}CH_3)]^+$ (M = Ti, Zr, Th) can occur in reaction media containing metallocene alkyl cations [7–10]. The presence of binuclear complexes has been inferred also from the effects of excess zirconocene dimethyl complex on the properties of catalyst systems containing $(CH_3)_2Si(indenyl)_2Zr(CH_3)_2$ and *n*-$Bu_3NH^+B(C_6F_5)_4^-$ [11]. Here, we present results of studies on NMR-spectral and catalytic properties of related reaction systems, aimed at a further characterization of binuclear zirconocene cations, at a delineation of the conditions under which they are formed and at a clarification of their effects on the properties of zirconocene catalyst systems.

2. Experimental

The zirconium complexes $(C_5H_5)_2ZrCl_2$ [12], $(CH_3)_4C_2(C_5H_4)_2ZrCl_2$ [13], $Me_2Si(C_5H_5)_2ZrCl_2$ [14,15], rac-$Me_2Si(ind)_2ZrCl_2$ [16,17], and $(C_5(CH_3)_5)_2ZrCl_2$ [18] were converted to the respective dimethyl compounds by reaction with 2 equivalents of CH_3Li in ether solution at −78°C; after warming to room temperature, the solutions were stirred for another 30 min and then evaporated to dryness. The dimethyl complexes were obtained by extraction with pentane and crystallization at low temperatures [19]. For the conversion of rac-Me_2Si(2-Me-benz[e]ind)$_2ZrCl_2$ [20,21] to the dimethyl derivative, this procedure was modified in that toluene was used as a solvent both for the reaction with CH_3Li and for the extraction of the dimethyl complex. $B(C_6F_5)_3$ was obtained as described by Pohlmann et al. [22]. All materials were kept and handled in a glovebox under N_2. C_6D_6 was purified by stirring over potassium metal, degassed, condensed onto a 4 Å molecular sieve and then stored in a glovebox under exclusion of light. Stock solutions containing 0.01 or 0.04 mol/L of each of the zirconium complexes or of $B(C_6F_5)_3$ in C_6D_6 were used for the preparation of the solutions studied.

^{1}H-NMR spectra of the solutions studied were measured on a Bruker WM-250 spectrometer. In a series of control experiments, hydrolysis and photolysis reactions of sample solutions were purposely induced. The absence of any signals assignable to the hydrolysis or photolysis products thus observed was used to monitor the integrity of the reactions systems investigated in this study.

The propene polymerization reactions were conducted under the conditions described in Ref. [10]; polymerization rates were measured by the rate of propene uptake. The rates shown in Figs. 5–7 represent maximal activities, which were reached, in general, 5–10 min after the start of each catalysis reaction.

3. Results

3.1. CH_3-bridged binuclear cations from zirconocene dimethyl complexes and $B(C_6F_5)_3$

Because of its NMR-spectral simplicity, we consider first the reaction system $(C_5H_5)_2Zr(CH_3)_2/B(C_6F_5)_3$ [23,24]. The ^{1}H-NMR signals expected for the contact ion pair $[(C_5H_5)_2ZrCH_3^+ \cdots H_3C\text{–}B(C_6F_5)_3^-]$ are observed in d_6-benzene solutions containing ca. 0.05 mol/L of $(C_5H_5)_2Zr(CH_3)_2$ and a slight excess of $B(C_6F_5)_3$ (B:Zr ≈ 1.2:1) (Fig. 1, Table 1): A singlet for the terminal CH_3 group at δ 0.28 ppm and a broad signal at δ 0.14 ppm for the Zr · · · CH_3–B bridge indicate that exchange between terminal and bridging CH_3 groups is slow on the NMR time scale. Higher exchange rates have been observed with related complexes at more elevated temperatures [25–27].

The signals of this ion pair decrease in intensity when $(C_5H_5)_2Zr(CH_3)_2$ is added at Zr:B ratios above 1:1. A new set of signals at δ 5.62, −0.12, and −1.19 ppm, with integrals in the

Table 1
^{1}H-NMR signals of dimethyl zirconocene complexes, their $B(C_6F_5)_3$ adducts, and of μ-CH_3-bridged binuclear cations, either solvent-separated from or associated with their $H_3C-B(C_6F_5)_3^-$ counter anions, in C_6D_6 (δ 7.15 ppm) at 25°C

Species\assignment	C_5H_5			Zr–CH_3	μ-CH_3	B–CH_3
$(C_5H_5)_2Zr(CH_3)_2$	5.70 (s, 10)			−0.12 (s, 6)		
$[(C_5H_5)_2ZrCH_3^+ \cdots H_3C-B(C_6F_5)_3^-]$	5.39 (s, 10)			0.28 (s, 3)		0.1 (b, 3)
$[((C_5H_5)_2ZrCH_3)_2(\mu\text{-}CH_3)^+] + H_3C-B(C_6F_5)_3^-$	5.62 (s, 20)			−0.12 (s, 6)	−1.19 (s, 3)	1.3 (b, 3)
$[((C_5H_5)_2ZrCH_3)_2(\mu\text{-}CH_3)^+ \cdots H_3C-B(C_6F_5)_3^-]$	5.52 (s, 20)			−0.19 (s, 6)	−1.36 (s, 3)	1.0 (b, 3)
Species\assignment	$C_5H_4(\beta)$	$C_5H_4(\alpha)$	$C_2(CH_3)_4$	Zr–CH_3	μ-CH_3	B–CH_3
$(CH_3)_4C_2(C_5H_4)_2Zr(CH_3)_2$	6.38 (pt, 4)	5.55 (pt, 4)	1.38 (s, 12)	−0.07 (s, 6)		
$[(CH_3)_4C_2(C_5H_4)_2ZrCH_3^+ \cdots H_3C-B(C_6F_5)_3^-]$	6.10,5.89 (pq, 2, 2)	5.59,5.09 (pq, 2, 2)	0.75,0.59 (s, 6, 6)	0.59 (s, 3)		0.4 (b, 3)
$[((CH_3)_4C_2(C_5H_4)_2ZrCH_3)_2(\mu\text{-}CH_3)^+] + H_3C-B(C_6F_5)_3^-$	n.r.	n.r.	n.r.	0.15 (s, 6)	−0.71 (s, 3)	1.3 (b, 3)
$[((CH_3)_4C_2(C_5H_4)_2ZrCH_3)_2(\mu\text{-}CH_3)^+ \cdots H_3C-B(C_6F_5)_3^-]$	n.r.	n.r.	n.r.	0.10 (s, 6)	−0.92 (s, 3)	1.0 (b, 3)
Species\assignment	$C_5H_4(\beta)$	$C_5H_4(\alpha)$	$(CH_3)_2Si$	Zr–CH_3	μ-CH_3	B–CH_3
$(CH_3)_2Si(C_5H_4)_2Zr(CH_3)_2$	6.68 (pt, 4)	5.41 (pt, 4)	−0.03 (s,6)	−0.12 (s,6)		
$[(CH_3)_2Si(C_5H_4)_2ZrCH_3^+ \cdots H_3C-B(C_6F_5)_3^-]$	6.32, 6.24 (pq, 2, 2)	5.29, 4.87 (pq, 2, 2)	−0.22, −0.04 (s, 3, 3)	0.32 (s, 3)		0.5 (b, 3)
$[((CH_3)_2Si(C_5H_4)_2ZrCH_3)_2(\mu\text{-}CH_3)^+] + H_3C-B(C_6F_5)_3^-$	n.r.	n.r.	n.r.	n.r.	−0.50 (s, 3)	1.3 (b, 3)
$[((CH_3)_2Si(C_5H_4)_2ZrCH_3)_2(\mu\text{-}CH_3)^+ \cdots H_3C-B(C_6F_5)_3^-]$	n.r.	n.r.	n.r.	n.r.	−0.90 (s, 3)	1.0 (b, 3)
Species\assignment	$C_5H_2(\beta)$	$C_5H_2(\alpha)$	$(CH_3)_2Si$	Zr–CH_3	μ-CH_3	B–CH_3
$(CH_3)_2Si(C_9H_6)_2Zr(CH_3)_2$	6.69 (d, 2)	5.68 (d, 2)	0.53 (s, 6)	−0.97 (s, 6)		
$[(CH_3)_2Si(C_9H_6)_2ZrCH_3^+ \cdots H_3C-B(C_6F_5)_3^-]$	6.57, 6.22 (d, 1, 1)	4.97, 5.67 (d, 1, 1)	0.21, 0.35 (s, 3, 3)	−0.51 (s, 3)		0.5 (b, 3)
$[((CH_3)_2Si(C_9H_6)_2ZrCH_3)_2(\mu\text{-}CH_3)^+]$	n.r.	n.r.	n.r.	−0.96 (s, 6) [a]	−2.90 (s, 3) [a]	1.4 (b, 3) [a]
$+H_3C-B(C_6F_5)_3^-$				−0.99 (s, 6) [a]	−3.10 (s, 3) [a]	1.4 (b, 3) [a]
$[((CH_3)_2Si(C_9H_6)_2ZrCH_3)_2(\mu\text{-}CH_3)^+ \cdots H_3C-B(C_6F_5)_3^-]$	n.r.	n.r.	n.r.	−1.23 (s, 6) [b]	−3.22 (s, 3) [b]	1.1 (b, 3) [b]
				−1.24 (s, 6) [b]	−3.40 (s, 3) [b]	1.1 (b, 3) [b]

s = singlet, d = doublet, pt = pseudotriplet, pq = pseudoquartet, b = broadened, n.r. = not resolved.
[a] Two species present in a ratio of 1.6 (top):1 (bottom).
[b] Two species present in a ratio of 1.8 (top):1 (bottom).

ratio of 20:6:3, indicates the presence of a binuclear cation $[((C_5H_5)_2ZrCH_3)_2(\mu\text{-}CH_3)]^+$: Shifts of terminal and bridging CH_3 groups are comparable to values of δ −0.56 and −1.59 ppm reported by Bochmann and coworkers [9] for a binuclear bisindenyl titanium methyl cation $[((ind)_2TiCH_3)_2(\mu\text{-}CH_3)]^+$ and δ 0.07 and −1.20 ppm reported by Marks and coworkers [7] for $[((C_5(CH_3)_5)_2ThCH_3)_2(\mu\text{-}CH_3)]^+$. For this latter complex, terminal and bridging CH_3 groups were found to exchange rapidly at room temperature; such an exchange is obviously slow for the binuclear zirconocene cation $[((C_5H_5)_2ZrCH_3)_2(\mu\text{-}CH_3)]^+$. The counter-anion $H_3C\text{–}B(C_6F_5)_3^-$, formed together with this binuclear cation, gives a broad singlet at δ 1.3 ppm. These and further data, to be discussed below, indicate the formation of a solvent-separated binuclear alkyl zirconocene cation according to equilibrium reaction (3).

$$\begin{aligned}&\left[(C_5H_5)_2Zr(CH_3)^+ \cdots H_3C\text{–}B(C_6F_5)_3^-\right]\\&\quad+(C_5H_5)_2Zr(CH_3)_2\\&\quad\rightleftharpoons\left[((C_5H_5)_2ZrCH_3)_2(\mu\text{-}CH_3)\right]^+\\&\qquad+H_3C\text{–}B(C_6F_5)_3^-\ \text{(solvent-separated)}.\end{aligned}\tag{3}$$

A still higher excess of $(C_5H_5)_2Zr(CH_3)_2$ does not cause the signals of this binuclear cation to grow any further (Fig. 1). Instead we observe, at Zr:B ratios above ca. 1.6:1, increasing proportions of another binuclear cation, likewise of composition $[((C_5H_5)_2ZrCH_3)_2(\mu\text{-}CH_3)]^+$, as indicated by its signals at δ 5.52, −0.19, and −1.32 ppm, again with an integral

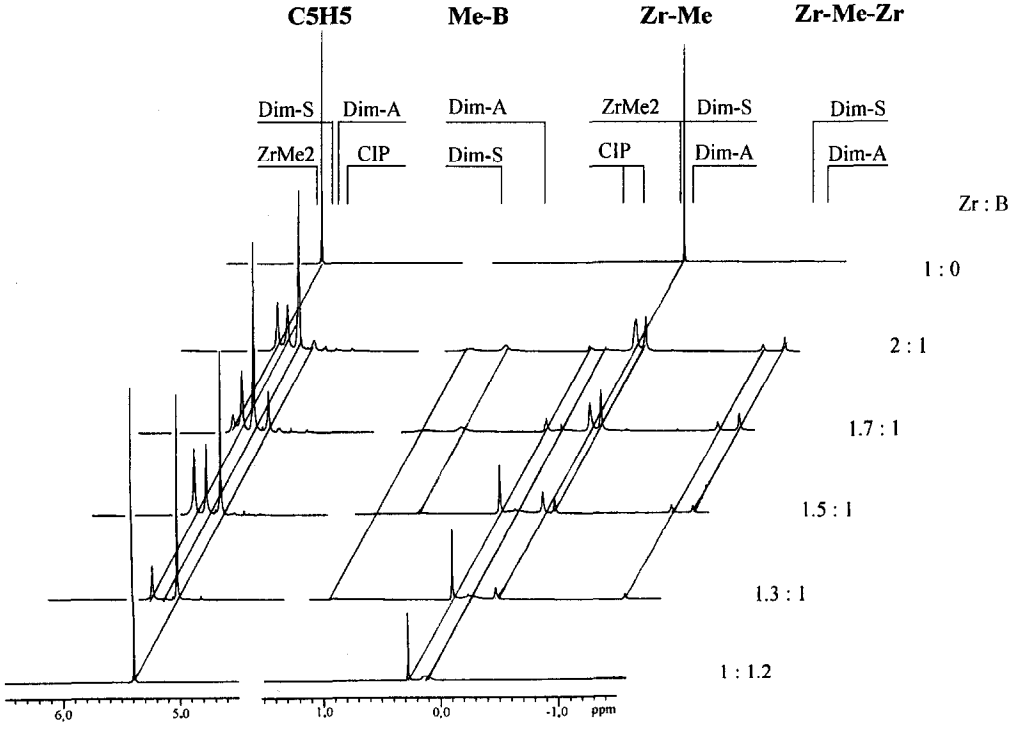

Fig. 1. ^{1}H-NMR spectra of C_6D_6 solutions containing $(C_5H_5)_2Zr(CH_3)_2$ and $B(C_6F_5)_3$ in different Zr:B ratios, at a constant total zirconocene concentration of $[Zr] = 4 \cdot 10^{-2}$ mol/L, at 25°C. Designation of zirconocene species involved: Dim-S, solvent-separated binuclear cation; Dim-A, associated binuclear ion pair; CIP, mononuclear contact ion pair; $ZrMe_2$, zirconocene dimethyl complex.

ratio of 20:6:3. This species becomes predominant in solutions with Zr:B ratios $\geq$ 1.7:1; here, the appearance of the signals of $(C_5H_5)_2$–$Zr(CH_3)_2$ at δ 5.70 and -0.12 ppm indicate that reaction (3) approaches completion.

An additional, broadened signal at δ 1.0 ppm associated with this second binuclear cation is assigned to its counter-anion H_3C–$B(C_6F_5)_3^-$. The chemical shift of this signal is close to that of δ 0.85 ppm observed for $Li^+ \cdots H_3C$–$B(C_6F_5)_3^-$ (generated by dissolving solid $LiCH_3$ and $B(C_6F_5)_3$ in C_6D_6), rather than to that of δ 1.3 ppm for the first of the binuclear species discussed above. This suggests that the species dominating at higher Zr:B ratios represents an associated ion pair containing the binuclear cation in contact with its borate counter-anion, $[((C_5H_5)_2ZrCH_3)_2(\mu\text{-}CH_3)^+ \cdots H_3C$–$B(C_6F_5)_3^-]$.

When solutions containing $(C_5H_5)_2Zr(CH_3)_2$ and $B(C_6F_5)_3$ in a ratio of Zr:B = 2:1 are diluted with C_6D_6, the signals of the solvent-separated binuclear cation gain in weight while those assigned to the associated species gradually diminish (Fig. 2). At total zirconocene concentrations of $[Zr]_{tot} \ll$ ca. 10^{-2} mol/L, as they are typically employed in zirconocene-catalyzed polymerization reactions, only the solvent-separated binuclear complex remains in significant concentrations.

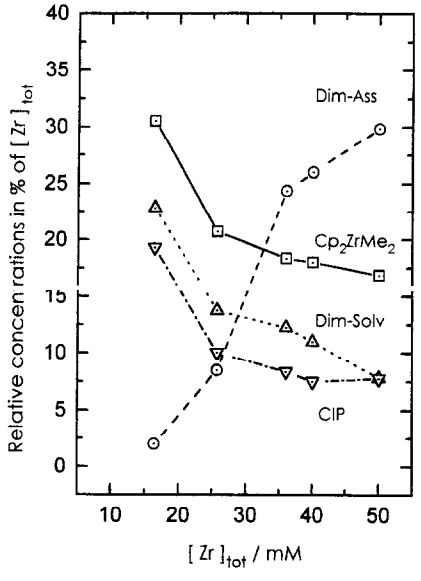

Fig. 2. Effects of total zirconocene concentration, [Zr], on the relative concentrations of $(C_5H_5)_2Zr(CH_3)_2$, of contact ion pairs $[C_5H_5)_2Zr(CH_3)^+ \cdots H_3C$–$B(C_6F_5)_3^-]$ and of solvent-separated and associated binuclear zirconocene cations, $[((C_5H_5)_2ZrCH_3)_2(\mu\text{-}CH_3)]^+$ H_3C–$B(C_6F_5)_3^-$ and $[((C_5H_5)_2ZrCH_3)_2(\mu\text{-}CH_3)^+ \cdots H_3C$–$B(C_6F_5)_3^-]$ at a [Zr]:[B] ratio of 2:1, in % of the total zirconocene concentration. Symbols as in Fig. 1.

As the signals of the individual species present under these conditions do not change over a period of up to one hour, we can assume that the individual complexes are in equilibrium with each other. As expected for equilibrium reaction (3), changes in total zirconocene concentrations leave the relative concentrations of the individual species practically unaffected (Fig. 2). From their relative ^{1}H-NMR intensities, we determine for this equilibrium a value of $K_3 = 1.0 \pm 0.2$. This value indicates that $(C_5H_5)_2Zr(CH_3)_2$ and H_3C–$B(C_6F_5)_3^-$ have similar Lewis basicities toward the cation $(C_5H_5)_2Zr(CH_3)^+$.

Efforts to obtain crystals of a binuclear zirconocene complex have not been successful so far. Solutions containing a 1:2 mixture of $B(C_6F_5)_3$ and a zirconocene dimethyl complex tend to deposit oily precipitates upon cooling or evaporation. When such a solution of $B(C_6F_5)_3$ and $(CH_3)_4C_2(C_5H_4)_2Zr(CH_3)_2$ in CH_2Cl_2 was slowly evaporated at -40°C, the oily precipitate contained some crystalline material. A crystal structure analysis showed that these crystals contained the mononuclear ion pair $[(CH_3)_4C_2(C_5H_4)_2Zr(CH_3)^+ \cdots H_3C$–$B(C_6F_5)_3^-]$ (Fig. 3, Table 2). Apparently, this species happens to crystallize more readily than the binuclear ion pair in equilibrium with it. The structure of this ion pair, especially the near-linear Zr–CH_3–B geometry, with three close Zr–H contacts, are in accord with previous studies on related ion-pair complexes [26,28].

For the bridging Zr–CH_3–Zr group of the binuclear $[((C_5H_5)_2ZrCH_3)_2(\mu\text{-}CH_3)]^+$ cation we find a coupling constant of $J(^1H, ^{13}C) = 136$ Hz in $CDCl_3$ solution at -45°C. Values of $J(^1H, ^{13}C) \approx 135$–$140$ Hz are typically observed for binuclear complexes with metal–

Table 2
Selected bond distances (in pm) and bond and dihedral angles (in degree) for the mononuclear ion pair complex $[(CH_3)_4C_2(C_5H_4)_2ZrCH_3^+ \cdots H_3C\text{-}B(C_6F_5)_3^-]$

Zr(1)–C(17)	251.6(8)	C(17)–B(1)	167.8(12)
Zr(1)–H(17A)	262.1	Zr(1)–H(17B)	237.5
Zr(1)–H(17C)	238.8	Zr(1)–C(18)	225.8(9)
Zr(1)–CR(1) [a]	218.1	Zr(1)–CR(2) [a]	218.4
Zr(1)–C(17)–B(1)	171.5(5)	C(17)–Zr(1)–C(18)	91.8(3)
CR(1)–Zr(1)–CR(2) [a]	125.1	PL(1)–Pl(2) [a]	56.6

[a] CR(1), CR(2), PL(1), PL(2): Centroids and mean planes of lower- and higher-numbered C_5 rings, respectively.

CH_3–metal bridges and indicate that the μ-CH_3 unit is close to a planar, sp^2-hybridized geometry [7,9,29].

With regard to the identity of the second CH_3-bridged species, the dependence of its concentration profile on total zirconocene concentration (Fig. 2) indicates that this species arises from an association of the type represented in Eq. (4), i.e. that it is an associated ion pair $[((C_5H_5)_2ZrCH_3)_2(\mu\text{-}CH_3)^+ \cdots H_3C\text{-}B(C_6F_5)_3^-]$. Alternative assignments, such as linear or cyclic tri- or tetranuclear complexes, appear incompatible with the observation of only one C_5H_5, terminal Zr–CH_3, μ-CH_3, and H_3C–$B(C_6F_5)_3^-$ signal each, with an integrated intensity ratio of 20:6:3:3 for these signals, and with the reagent ratios required to generate this species.

Our data are in accord with an equilibrium constant $K_4 = (0.45 \pm 0.1) \cdot 10^3\ (mol/L)^{-1}$ for

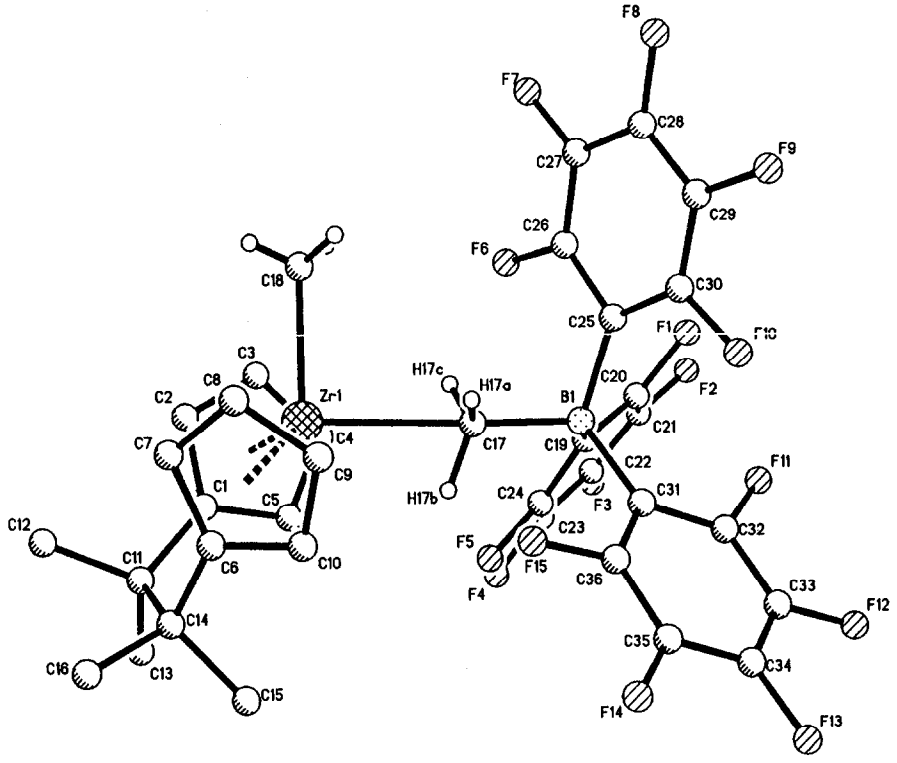

Fig. 3. Crystal structure of the ion pair $[(CH_3)_4C_2(C_5H_4)_2ZrCH_3^+ \cdots H_3C\text{-}B(C_6F_5)_3^-]$. Crystal data: $C_{36}H_{26}BF_{15}Zr$; *a* 29.522(12), *b* 10.041(4), *c* 23.738(10) Å, β 111.42(3)°; *V* 6550(5) Å^3; monoclinic, space group C2/c; *Z* 8; D_{calc} 2.238 g/cm^3; Mo Kα radiation (λ 0.71073 Å); μ 0.439 mm^{-1}; F(000) 3376; *T* 235 K; crystal size 0.3 · 0.3 · 0.4 mm; data collection on a Siemens R3m/V diffractometer; structure solution and refinement with Siemens SHELXTL PLUS (VMS) software (Patterson method); hydrogen atoms calculated and refined using the riding model technique with fixed isotropic U, except for Zr–CH_3 hydrogen atoms, which were found by difference Fourier analysis and refined isotropically; non-H atoms refined anisotropically with full-matrix least-squares technique; final *R* 0.0524, R_w 0.0489, *S* 1.27; residual electron density with largest difference peak 0.51 e Å^{-3}, largest difference hole −0.46 e Å^{-3}. Further structure parameters are available upon request from Fachinformations-Zentrum Karlsruhe, Eggenstein-Leopoldshafen, D-76344, upon quotation of the Journal reference, the authors and the deposit number CSD-59314 of this article.

the formation of the associated ion pair according to Eq. (4). Such an associated ion pair will be of significance only at catalyst concentrations above ca. 10^{-4} mol/L (Scheme 1).

$$[((C_5H_5)_2ZrCH_3)_2(\mu\text{-}CH_3)]^+ + H_3C\text{–}B(C_6F_5)_3^- \text{ (solvent-separated)} \rightleftharpoons [((C_5H_5)_2ZrCH_3)_2(\mu\text{-}CH_3)^+ \cdots H_3C\text{–}B(C_6F_5)_3^-] \text{ (associated)}. \quad (4)$$

With regard to the binding of the H_3C–$B(C_6F_5)_3^-$ anion in such an associated ion pair, our data do not allow to distinguish between a fluctuation of the H_3C–$B(C_6F_5)_3^-$ anion and a symmetrical bonding of the H_3C–$B(C_6F_5)_3^-$ anion to both Zr centers, which would then acquire a formal coordination number of 5. At any rate, this association is weak enough to allow the binuclear cation $[((C_5H_5)_2ZrCH_3)_2(\mu\text{-}CH_3)]^+$ to exist as a solvent-separated entity in more dilute solutions, whereas no signs for the formation of solvent-separated species are detectable for the mononuclear ion pair $[(C_5H_5)_2Zr(CH_3)^+ \cdots H_3C\text{–}B(C_6F_5)_3^-]$. The binuclear cation $[((C_5H_5)_2ZrCH_3)_2(\mu\text{-}CH_3)]^+$ thus appears to be much less electrophilic than the putative mononuclear cation $[(C_5H_5)_2Zr(CH_3)]^+$, which is most likely incapable of existing *per se*.

Similar results were obtained with the ring-bridged zirconocene complexes $(CH_3)_4C_2(C_5H_4)_2Zr(CH_3)_2$ and $(CH_3)_2Si(C_5H_4)_2Zr(CH_3)_2$: A slight excess of $B(C_6F_5)_3$ generates signals of a mononuclear species $[(CH_3)_4C_2(C_5H_4)_2ZrCH_3^+ \cdots H_3C\text{–}$

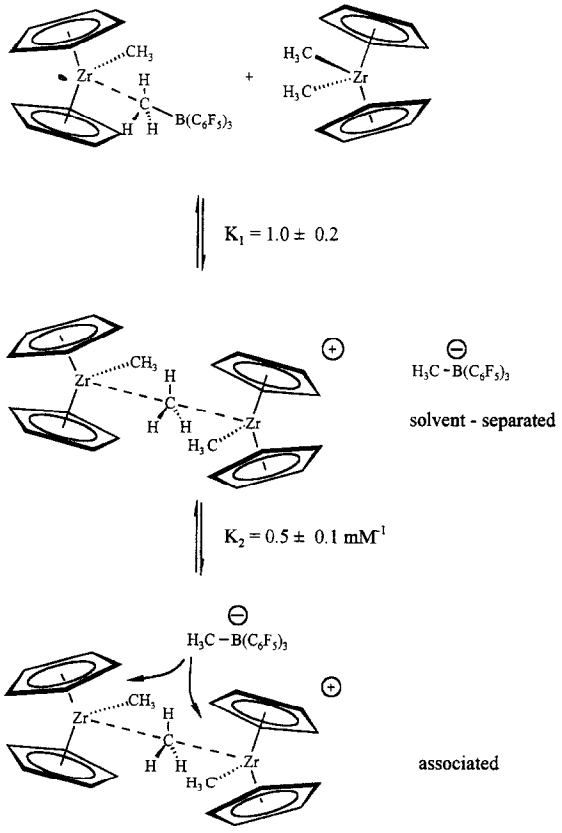

Scheme 1. Scheme 1Formation of binuclear zirconocene cations $[((C_5H_5)_2ZrCH_3)_2(\mu\text{-}CH_3)^+]$, in solvent-separated and associated ion pairs with the anion H_3C–$B(C_6F_5)_3^-$, in equilibria between the mononuclear ion pair $[(C_5H_5)_2ZrCH_3^+ \cdots H_3C\text{–}B(C_6F_5)_3^-]$ and dimethyl zirconocene, $(C_5H_5)_2Zr(CH_3)_2$, observed in C_6D_6 solution at 25°C.

$B(C_6F_5)_3^-$] and of its Me_2Si-bridged congener $[(CH_3)_2Si(C_5H_4)_2ZrCH_3^+ \cdots H_3C{-}B(C_6F_5)_3^-]$ (Table 1). Four separate ring hydrogen and two separate $(CH_3)_4C_2$ and $(CH_3)_2Si$ signals indicate that CH_3 and $H_3C{-}B(C_6F_5)_3$ ligands do not exchange coordination sites rapidly in these complexes at room temperature.

An increasing excess of $(CH_3)_4C_2(C_5H_4)_2Zr(CH_3)_2$ over $B(C_6F_5)_3$ generates Zr–(μ-CH_3)–Zr signals at δ −0.71 and −0.92 ppm for $(CH_3)_4C_2$-bridged and at −0.50 and −0.90 ppm for $(CH_3)_2Si$-bridged complexes. Broadened $H_3C{-}B(C_6F_5)_3^-$ signals at δ +1.3 and +1.0 ppm are typical, in both reaction systems, for the solvent-separated and associated pairs of binuclear cations and $H_3C{-}B(C_6F_5)_3^-$ anions, respectively, as discussed above. Other signals of these complexes are not well resolved; their detailed interpretation is thwarted by superposition of multiple signal sets due to several species in the region between 5 and 6.5 ppm.

Essentially analogous observations are made with the reaction system rac-$Me_2Si(ind)_2Zr(CH_3)_2/B(C_6F_5)_3$ (Table 1). As previously observed by Bochmann and coworkers in CD_2Cl_2 solution at −60°C [9], a doubling of the number of their ^{1}H-NMR signals indicates the formation of diastereomeric dimers from R- and S-configurated ansa–metallocene units. Even for these substituted ansa–metallocene systems, we observe comparable amounts of solvent-separated and of associated binuclear cations in $2.7 \cdot 10^{-2}$ M solutions in C_6D_6 at 25°C. Estimates of $K_3 \approx 2$ and of $K_4 \approx 0.8 \cdot 10^3$ $(mol/L)^{-1}$ indicate that the formation of these binuclear cations is affected only in a minor way by the introduction of indenyl instead of cyclopentadienyl ligands.

With the permethylated complex $(C_5(CH_3)_5)_2Zr(CH_3)_2$, on the other hand, we observe only the formation of a $B(C_6F_5)_3$ adduct, i.e. of the mononuclear contact ion pair $[(C_5(CH_3)_5)_2ZrCH_3^+ \cdots H_3C{-}B(C_6F_5)_3^-]$ with signals at δ 1.38, 0.30, and −0.16 ppm, with an integrated intensity ratio of 30:3:3. Even in the presence of excess $(C_5(CH_3)_5)_2Zr(CH_3)_2$, only the signals of this $B(C_6F_5)_3$ adduct are apparent, together with those of $(C_5(CH_3)_5)_2Zr(CH_3)_2$ at δ 1.76 and −0.55 ppm. Signals assignable to a binuclear cation are not detectable under these conditions. A binuclear cation, analogous to the thorium complex $[((C_5(CH_3)_5)_2ThCH_3)_2(\mu\text{-}CH_3)]^+$ [7], is apparently incompatible with the small size of the Zr(IV) center vis-a-vis the steric demands of the permethylated ring ligands. Similarly, no signals assignable to a binuclear cation are observed in the reaction system rac-Me_2Si(2-Me-benz[e]ind)$_2Zr(CH_3)_2/B(C_6F_5)_3$. Here, again, the steric demands of the extended benzindenyl ligand system appear to prevent the close approach of two Zr centers required for the formation of a CH_3-bridged binuclear cation.

3.2. Polymerization of propene with the catalyst system $Me_2Si(Ind)_2Zr(CH_3)_2$ / n-$Bu_3NH^+B(C_6F_5)_4^-$

The kinetics of propene polymerization in the catalyst system formed from rac-dimethylsilyl-bis(indenyl)zirconium dimethyl and the cation-generating reagent tris-*n*-butylammonium tetrakis(pentafluorophenyl) borate was investigated, especially with regard to the dependence of the rate of polymerization on the catalyst concentration, the dimethyl-metallocene/ammonium-borate ratio and the polymerization temperature. In this way, we have tried to clarify how the formation of the binuclear zirconocene cation $[(Me_2Si(Ind)_2ZrCH_3)_2(\mu\text{-}CH_3)]^+$ affects the catalytic activity in these reaction systems.

3.3. Effects of the total catalyst concentration on the rate of propene polymerization

Fig. 4 represents the rate of polymerization as a function of the initial catalyst concentration, determined at a 1:1 ratio of dimethyl metallocene to ammonium borate. It is apparent that a small change in concentration causes a remarkable increase in the rate of polymerization. Cat-

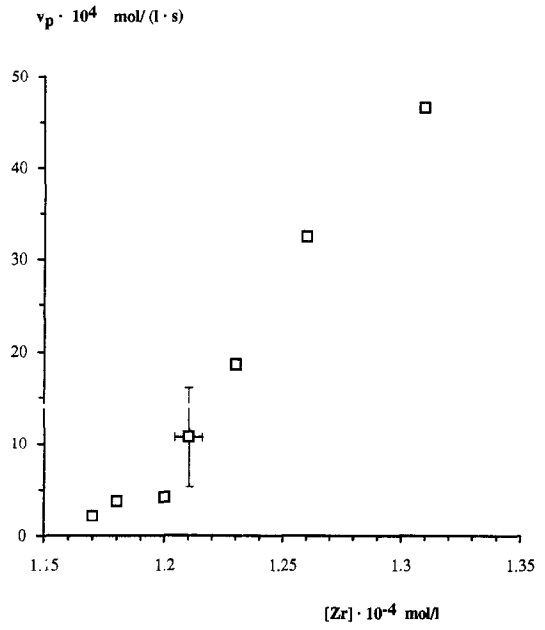

Fig. 4. Rates of propene polymerization, v_p, as a function of total zirconium concentration, [Zr]. Polymerization conditions: Dimethyl-zirconocene:ammonium-borate ratio [Zr]:[B] = 1:1; $Me_2Si(ind)_2Zr(CH_3)_2$ and $Bu_3NH^+B(C_6F_5)_4^-$ prereacted for 35 min in 5 ml toluene; p(propene) = 2 bar; T_p = 25°C, in toluene solution.

alyst concentrations below a certain threshold value afford no activity at all. This indicates that the catalyst system is totally deactivated up to a limiting catalyst concentration, presumably by impurities. This deactivation is, in fact, directly observable by a decoloration of the light yellow reaction mixture of dimethyl metallocene and ammonium borate after its injection into the solvent-filled reactor.

The limiting catalyst concentration, which just allows a significant polymerization activity to be observed, must depend on the purity of all substances used as well as on the cleanliness of the reactor system. For the present series of experiments, it has a value of ca. $1.15 \cdot 10^{-4}$ mol/L. This quantity corresponds to a sacrificial consumption, either of $Me_2Si(ind)_2Zr(CH_3)_2$ or of an ion-pair complex such as $[Me_2Si(Ind)_2ZrCH_3^+ \cdots B(C_6F_5)_4^-]$, which is required to free the reaction system of adventitious inhibitors.

That the catalytically active species *per se* is highly reactive is apparent from the strong increase in activities observed when catalyst concentrations are increased above the limiting value. At total catalyst concentrations exceeding $1.3 \cdot 10^{-4}$ mol/L activities are so high that the temperature of the reaction system becomes difficult to control. Reproducible rate measurements are thus limited to catalyst concentrations in the narrow range between 1.15 and $1.3 \cdot 10^{-4}$ mol/L.

3.4. Effects of the ammonium-borate / dimethyl-metallocene ratio on the rate of propene polymerization

In this series of experiments, catalytic activities were determined at a constant initial $Me_2Si(ind)_2Zr(CH_3)_2$ concentration of $1.31 \cdot 10^{-4}$ mol/L and varying concentrations of *n*-$Bu_3NH^+B(C_6F_5)_4^-$ (Fig. 5). It is apparent that incomplete addition of ammonium borate as well as its addition in excess over metallocene has a negative effect on the rate of polymerization, which goes through a maximum close to

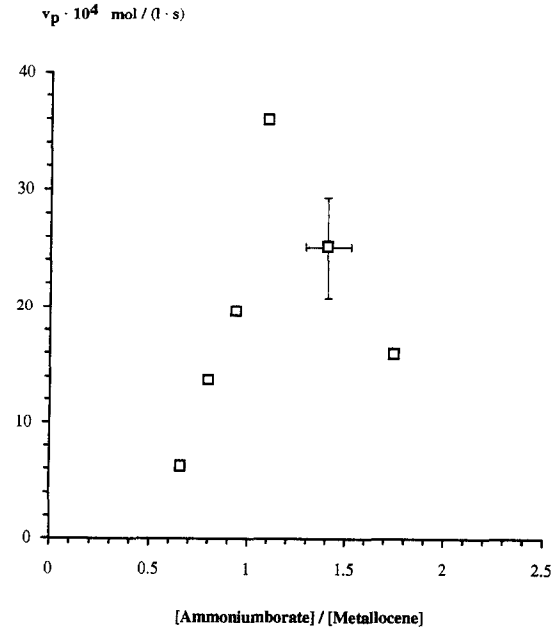

Fig. 5. Rates of propene polymerization, v_p, as a function of the ammonium-borate:dimethyl-zirconocene ratio [B]:[Zr]. Polymerization conditions: Total zirconocene concentration constant at [Zr] = $1.31 \cdot 10^{-4}$ mol/L; otherwise as in Fig. 4.

an equimolar ratio of the two catalyst components.

The shape of the curve in Fig. 5 shows that decreased concentrations of ammonium borate result in an over-proportional decrease in the rates of polymerization. This effect is most likely caused by the fact that under these conditions the absolute concentrations of catalyst are decreased to and finally beyond the minimal threshold value discussed above. Only the excess of metallocene present in these cases explains that finite polymerization activities are still observable at these low catalyst concentrations, where a 1:1 mixture of ammonium borate and dimethyl metallocene would result in no activities at all.

The loss of polymerization rate caused by an excess of cation-generating reagent, on the other hand, could be explained either by a deactivating interaction of the tetrakis(perfluorophenyl)borate anion with the metallocene cation [9] or, possibly, by a protolytic elimination of the second Zr – bound methyl group by excess tributyl ammonium ion.

3.5. *Effects of the dimethyl-metallocene / ammonium-borate ratio on the rate of propene polymerization*

In this series, the initial concentration of n-$Bu_3NH^+B(C_6F_5)_4^-$ was kept constant at $8.5 \cdot 10^{-5}$ mol/L; $Me_2Si(ind)_2Zr(CH_3)_2$ was added in excess with Zr:B ratios in the range of 1:1 to 4:1. From Fig. 6 it is evident that a measurable rate of polymerization requires at least a Zr:B ratio of 1.2:1, i.e. an absolute zirconocene concentration close to the threshold value determined above. Beyond this Zr:B ratio, the rate of polymerization increases steadily with increasing excess of dimethyl metallocene.

The activity increase up to a Zr:B ratio of 2.2:1 is explained by the sacrificial consumption of ca. $1.1 \cdot 10^{-4}$ mol/L of $Me_2Si(ind)_2Zr(CH_3)_2$ for the removal of some inhibitor(s) and the subsequent stoichiometric generation of the catalytically active contact ion pair $[Me_2Si(Ind)_2ZrCH_3^+ \cdots B(C_6F_5)_4^-]$ from equimolar amounts of dimethyl metallocene and cation-generating reagent. As these reactions are complete at a Zr:B ratio of ca. 2.2:1, activities would be expected to level off at higher dimethyl-metallocene/ammonium-borate ratios. The continued activity increase observed at Zr:B ratios up to 3.6:1 thus requires another explanation.

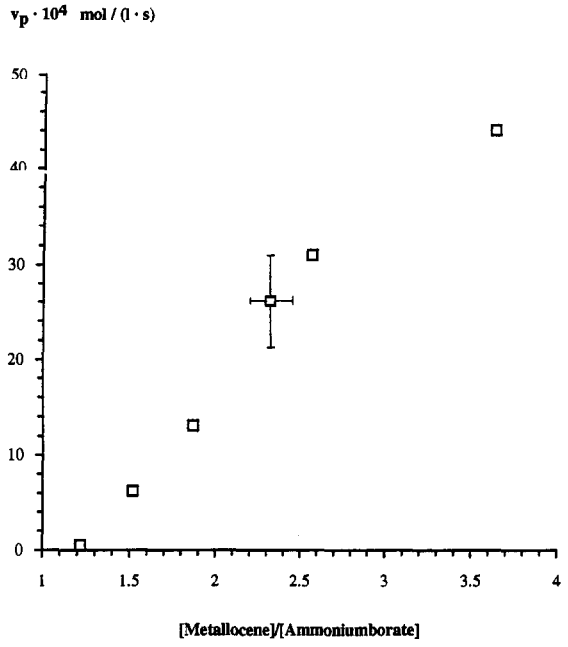

Fig. 6. Rates of propene polymerization, v_P, as a function of the dimethyl-zirconocene:ammonium-borate ratio, [Zr]:[B]. Polymerization conditions: Concentration of (n- $Bu)_3NH^+B(C_6F_5)_4^-$ constant at $[B] = 8.5 \cdot 10^{-5}$; otherwise as in Fig. 4.

From preceding studies [7–10] and from our present ^{1}H-NMR data on this reaction system it is clear that an excess of dimethyl metallocene will induce formation of the binuclear, cationic metallocene complex $[(Me_2Si(Ind)_2ZrCH_3)_2(\mu\text{-}CH_3)]^+$. Although the anion $B(C_6F_5)_4^-$ instead of $H_3C\text{–}B(C_6F_5)_3^-$ represents the counter-anion in the contact ion pair $[Me_2Si(ind)_2ZrCH_3^+ \cdots B(C_6F_5)_4^-]$ generated in this system, a binuclear cation $[Me_2Si(ind)_2ZrCH_3)_2(\mu\text{-}CH_3)]^+$ identical to that discussed above will certainly be formed by excess $Me_2Si(ind)_2Zr(CH_3)_2$ from this contact ion pair. As the zirconocene concentrations in these catalyst systems are only ca.

10^{-4} mol/L, association of the binuclear cation with its counter-anion is unlikely to be of any significance. We can thus assume that equilibrium reaction (5) describes the species present, before the addition of olefin, in reaction systems containing an excess of $Me_2Si(ind)_2Zr(CH_3)_2$.

$$\left[Me_2Si(Ind)_2ZrCH_3^+ \cdots B(C_6F_5)_4^-\right] + Me_2Si(Ind)_2Zr(CH_3)_2 \rightleftharpoons \left[(Me_2Si(Ind)_2ZrCH_3)_2(\mu\text{-}CH_3)\right]^+ + B(C_6F_5)_4^- \quad (5)$$

The question then arises whether such a binuclear cation might represent an additional catalyst species, which induces polymer growth at a higher rate than a mononuclear cation. This hypothesis is not supported, however, by the analytical data of the polymers produced with these catalyst systems: Their molar masses and mass distributions as well as their isotacticities remain invariant against the variation of the dimethyl-metallocene/ammonium-borate ratio in this series of experiments (Tables 3 and 4). This indicates that only a single catalyst species contributes to polymer formation, irrespective of the dimethyl-metallocene/ammonium-borate ratio used. The mononuclear zirconocene cation formed from equimolar amounts of dimethyl metallocene and ammonium borate thus appears to remain the sole catalyst species even at higher dimethyl-metallocene/ammonium-borate ratios.

Table 3
Melting points, T_m [a], isotacticities [b], and 2,1-misinsertion frequencies [c] of polypropene samples obtained at various dimethyl-zirconocene:ammonium-borate ratios [d]

[Zr] (mol/L·10^{-4})	[Zr]:[B]	T_m (°C)	Isotacticity (%)	m-2.1 (%)
1.24	1:1.45	149.3	95.6	0.5
1.24	1:1	149.1	95.4	0.4
1.29	1.52:1	149.3	96.3	0.4
2.18	2.57:1	149.9	95.4	0.4
3.09	3.64:1	149.0	96.2	0.4

[a] Determined by DSC, in °C.
[b] mmmm pentad ^{13}C signal integral relative to sum of all pentad signal integrals, in %.
[c] One eighth of the sum of the integrals of the 2,1-misinsertion ^{13}C signals at 17.1, 17.5, 30.4, 31.4, 35.7, 35.8, 38.4, and 42.1 ppm relative to sum of all pentad signal integrals, in %.
[d] Polymerization conditions: $Me_2Si(ind)_2Zr(CH_3)_2$ and $(n\text{-}Bu)_3NH^+B(C_6F_5)_4^-$ prereacted for 35 min in 5 ml toluene; p(propene) = 2 bar; T_P = 25°C, in toluene solution, total volume 150 ml.

Table 4
Molar masses of polypropene samples obtained at various dimethyl-zirconocene:ammonium-borate ratios [a]

[Zr]:[B]	M_w	M_n	M_w/M_n
1.52:1	95100	57800	1.65
1.87:1	97500	65100	1.50
2.32:1	99000	52000	1.92
2.57:1	102300	77500	1.64
3.64:1	99800	61800	1.61

[a] Polymerization conditions: $Me_2Si(ind)_2Zr(CH_3)_2$ and $(n\text{-}Bu)_3NH^+B(C_6F_5)_4^-$ prereacted for 35 min in 5 ml toluene; $c((n\text{-}Bu)_3NH^+B(C_6F_5)_4^-) = 8.5 \cdot 10^{-5}$ mol/L; otherwise as in Table 3.

At any rate, binuclear cations of the type $[(Me_2Si(Ind)_2ZrCH_3)_2(\mu\text{-}CH_3)]^+$ do not appear to contribute in any way to chain growth termination, as the molar mass of the polymer products remains unchanged in the presence of excess $Me_2Si(Ind)_2Zr(CH_3)_2$, i.e. under conditions where these binuclear cations are the predominant species.

The beneficial effects which the formation of a binuclear cation such as $[(Me_2Si(Ind)_2ZrCH_3)_2(\mu\text{-}CH_3)]^+$ is found to have on the activities of these catalyst systems might instead result from an increased stability of the catalyst system against deactivation. Reaction of the mononuclear ion pair with dimethyl metallocene according to Eq. (5) is likely to decrease the strong electrophilicity of the metallocene cation. Such a species might thus be stabilized against deactivating side reactions, while still being an efficient source of the reactive cationic olefin complex $[Me_2Si(Ind)_2ZrCH_3 \cdots (C_3H_6)]^+$ according to Eq. (6).

$$\left[(Me_2Si(Ind)_2ZrCH_3)_2(\mu\text{-}CH_3)\right]^+ + C_3H_6 \rightleftharpoons \left[Me_2Si(Ind)_2ZrCH_3(C_3H_6)\right]^+ + Me_2Si(Ind)_2Zr(CH_3)_2. \quad (6)$$

While an increase in the steady-state concentration of the essential polymer-bearing cation $[Me_2Si(Ind)_2Zr(Pol)]^+$ is likely to be caused by its protective association with

$Me_2Si(Ind)_2Zr(CH_3)_2$, a net increase in the rate of polymerization is to be expected only if this stabilizing effect outweighs the reduced tendency of the resulting binuclear complex to form the 'productive' cation $[Me_2Si(Ind)_2Zr(Pol)(C_3H_6)]^+$ by coordination of propene. Observations by Bochmann and Lancaster [30] on the reduced stability of binuclear cations with μ-ethyl instead of μ-methyl bridges suggest that increasing lengths of the Zr-bound polymer chain will indeed render the resulting binuclear species increasingly prone to cleavage by an olefin. In the absence of any direct information on the equilibrium constants for the reactions involved, i.e. of equilibria analogous to reactions (5) and (6) but with a polymer chain in place of the Zr-bound methyl group, we must forgo a more detailed analysis of the ways in which the formation of binuclear cations brings about the increase in polymerization rates represented in Fig. 6. It appears certain, however, that the increased rate of polymerization caused by an excess of $Me_2Si(Ind)_2Zr(CH_3)_2$ in the reaction system is due to some protective effects associated with the presence of binuclear, alkyl-bridged cations.

3.6. Effects of the polymerization temperature on the rate of propene polymerization

Rates of propene polymerization with $Me_2Si(Ind)_2Zr(CH_3)_2/n\text{-}Bu_3NH^+B(C_6F_5)_4^-$ were determined, in toluene solution at 2 bar propene pressure, at varying polymerization temperatures. Fig. 7 shows a strong decrease of the rates of polymerization in the region between 15 and 45°C; at 55°C activities had totally disappeared.

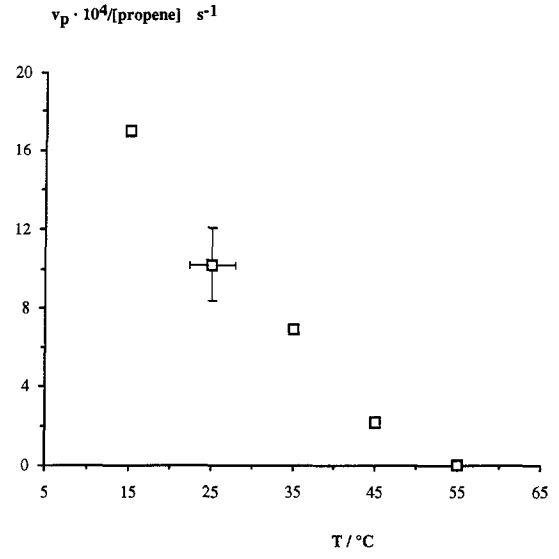

Fig. 7. Rates of propene polymerization, v_P, as a function of the polymerization temperature, T_P. Polymerization conditions: Total zirconocene concentration constant at $[Zr] = 1.20 \cdot 10^{-4}$ mol/L; dimethyl-zirconocene:ammonium-borate ratio [Zr]:[B] = 1:1; $Me_2Si(ind)_2Zr(CH_3)_2$ and $Bu_3NH^+B(C_6F_5)_4^-$ prereacted for 30 min in 7 ml toluene; p(propene) = 2 bar; in toluene solution.

The analytical data of the polymers obtained at these temperatures show the expected decrease in molar mass but rather constant molar mass dispersities and microstructures (Tables 5 and 6). This indicates that the species responsible for polymer growth remain the same in this temperature range.

Table 5
Melting points, T_m [a], relative pentad intensities [b], and 2,1-misinsertion frequencies [c] of polypropene samples obtained at various polymerization temperatures [d]

T_p (°C)	T_m (°C)	mrrm (%)	mmrr (%)	mmmr (%)	mmmm (%)	m-2.1 (%)
5	154.0	0.5	0.9	1.0	97.7	0.32
15	151.8	0.6	1.2	1.2	97.1	0.38
25	149.0	0.7	1.6	1.7	96.1	0.41
35	147.1	1.0	2.1	2.0	95.1	0.44

[a] Determined by DSC, in °C.
[b] Pentad ^{13}C signal integral relative to sum of all pentad signal integrals, in %.
[c] One eigths of the sum of the integrals of the 2,1-misinsertion ^{13}C signal at 17.1, 17.5, 30.4, 31.4, 35.7, 35.8, 38.4, and 42.1 ppm relative to sum of all pentad signal integrals, in %.
[d] Polymerization conditions: $Me_2Si(ind)_2Zr(CH_3)_2$ and $(n\text{-}Bu)_3NH^+B(C_6F_5)_4^-$ prereacted for 30 min in 7 ml toluene; total zirconocene concentration in the reaction mixture, $[Zr] = 1.21 \cdot 10^{-4}$ mol/L; [Zr]:[B] = 1:1; otherwise as in Table 3.

Table 6
Molar masses of polypropene samples obtained at various polymerization temperatures [a]

T_p (°C)	M_w	M_n	M_w / M_n
5	167800	95500	1.76
10	144000	83600	1.72
15	134200	73100	1.84
25	96300	57000	1.69
35	76000	44900	1.69

[a] Polymerization conditions as given in Table 5.

The reason for the decrease of activity is undoubtedly the thermal instability of the catalyst system. Again, the deactivation is directly observable by the decoloration of the light yellow reaction solution in the reactor. At a reaction temperature of 55°C the pre-reacted orange–brown catalyst solution is decolored immediately after injection into the solvent-filled reactor; at 45°C a weak light yellow coloration remains only for a few minutes. At 15°C, a decrease in color intensity is practically undetectable. These observations underline that the overall activities accessible for these 'cationic' catalysts are crucially limited by their susceptibility to deactivation. Activities in these catalyst systems are thus likely to benefit from the stabilizing effects associated with the formation of less electrophilic binuclear cations.

Acknowledgements

This work was supported by BMBF and by BASF AG.

References

[1] R.F. Jordan, C.S. Bajgur, R. Willett and B. Scott, J. Am. Chem. Soc. 108 (1986) 7410; R.F. Jordan, Adv. Organomet. Chem. 32 (1991) 325.
[2] G.G. Hlatky, D.J. Upton and H.W. Turner, US Pat. Appl. 459921 (1990); Chem. Abstr. 115 (1991) 256897v.
[3] M. Bochmann and S.J. Lancaster, Organometallics 12 (1993) 633.
[4] J.C.W. Chien, W.M. Tsai and M.D. Rausch, J. Am. Chem. Soc. 113 (1991) 8570.
[5] J.J. Eisch, S.I. Pombrik and G.X. Zheng, Organometallics 12 (1993) 3856; Makromol. Chem., Macromol. Symp. 66 (1993) 109.
[6] X. Yang, C.L. Stern and T.J. Marks, Angew. Chem. Int. Ed. Engl. 31 (1992) 1375; C. Sishta, R.M. Hathorn and T.J. Marks, J. Am. Chem. Soc. 114 (1992) 1112.
[7] X. Yang, C.L. Stern and T.J. Marks, Organometallics 10 (1991) 840.
[8] G.G. Hlatky and H.W. Turner, private communication.
[9] M. Bochmann and S.J. Lancaster, J. Organomet. Chem. 434 (1992) C1; Angew. Chem. Int. Ed. Engl. 33 (1994) 1634; M. Bochmann, Angew. Chem. Int. Ed. Engl. 31 (1992) 1181.
[10] T. Haselwander, S. Beck and H.H. Brintzinger, in: Ziegler Catalysts, ed. G. Fink, R. Mülhaupt and H.H. Brintzinger (Springer-Verlag, Berlin, 1995) p. 181.
[11] N. Herfert and G. Fink, Makromol. Chem. Rapid Commun. 14 (1993) 91.
[12] B. Heyn, B. Hipler, G. Kreisel, H. Schreer and D. Walther, Anorganische Synthesechemie – Ein Integriertes Praktikum (Springer-Verlag, Berlin, 1986) p. 84.
[13] H. Schwemlein and H.H. Brintzinger, J. Organomet. Chem. 254 (1983) 69.
[14] N. Klouras and H. Köpf, Monatsh. Chem. 112 (1981) 887.
[15] C.S. Bajgur, W.R. Tikkanen and J.L. Petersen, Inorg. Chem. 24 (1985) 2539.
[16] J.A. Ewen, L. Haspeslagh, M.J. Elder, J.L. Atwood, H. Zhang and H.N. Cheng, in: Transition Metals and Organometallics as Catalysts for Olefin Polymerization, ed. W. Kaminsky and H. Sinn (Springer Verlag, Berlin, 1988) p. 281.
[17] W.A. Herrmann, J. Rohrmann, E. Herdtweck, W. Spaleck and A. Winter, Angew. Chem. Int. Ed. Engl. 28 (1989) 1511.
[18] J.M. Manriquez, D.R. McAlister, E. Rosenberg, A.M. Shiller, K.L. Williamson, S.I. Chan and J.E. Bercaw, J. Am. Chem. Soc. 100 (1978) 3078.
[19] E. Samuel and M.D. Rausch, J. Am. Chem. Soc. 95 (1973) 6263.
[20] W. Spaleck, F. Küber, A. Winter, J. Rohrmann, B. Bachmann, M. Antberg, V. Dolle and E.F. Pauls, Organometallics 13 (1994) 954.
[21] U. Stehling, J. Diebold, R. Kirsten, W. Röll, H.H. Brintzinger, S. Jüngling, R. Mülhaupt and F. Langhauser, Organometallics 13 (1994) 964.
[22] J.L.W. Pohlmann, F.E. Brinckman, G. Tesi and R.E. Donadio, Z. Naturforschg. 20b (1965) 1; J.L.W. Pohlmann and F.E. Brinckman, Z. Naturforschg. 20b (1965) 5.
[23] M.J. Elder and J.A. Ewen, US Pat. Appl. 419057 (1989); Chem. Abstr. 115 (1991) 136998g.
[24] X. Yang, C.L. Stern and T.J. Marks, J. Am. Chem. Soc. 113 (1991) 3623.
[25] A.R. Siedle and R.A. Newmark, J. Organomet. Chem. 497 (1995) 119.
[26] X. Yang, C.L. Stern, T.J. Marks, J. Am. Chem. Soc. 116 (1994) 10015.
[27] P.A. Deck and T.J. Marks, J. Am. Chem. Soc. 117 (1995) 6128.
[28] M. Bochmann, S.J. Lancaster, M.B. Hursthouse, K.M. Abdul Malik, Organometallics 13 (1994) 2235.
[29] R.M. Waymouth, B.D. Santarsiero, R.J. Coots, M.J. Bronikowski and R.H. Grubbs, J. Am. Chem. Soc. 108 (1986) 1427.
[30] M. Bochmann and S.J. Lancaster, J. Organomet. Chem. 497 (1995) 55.